

# Multivariate analysis of diffusion tensor imaging data improves the detection of microstructural damage in young professional boxers

Michael H. Chappell<sup>a,d,\*</sup>, Jennifer A. Brown<sup>b</sup>, John C. Dalrymple-Alford<sup>c,d</sup>,  
Aziz M. Uluğ<sup>e</sup>, Richard Watts<sup>a,d</sup>

<sup>a</sup>Department of Physics and Astronomy, University of Canterbury, Christchurch 8020, New Zealand

<sup>b</sup>Department of Mathematics and Statistics, University of Canterbury, Christchurch 8020, New Zealand

<sup>c</sup>Department of Psychology, University of Canterbury, Christchurch 8020, New Zealand

<sup>d</sup>Van der Veer Institute for Parkinson's and Brain Research, Christchurch 8001, New Zealand

<sup>e</sup>Department of Radiology, Weill Medical College of Cornell University, New York, NY 10021, USA

Received 11 January 2008; revised 11 April 2008; accepted 11 April 2008

## Abstract

In this study, we present two different methods of multivariate analysis of voxel-based diffusion tensor imaging (DTI) data, using as an example data derived from 59 professional boxers and 12 age-matched controls. Conventional univariate analysis ignores much of the diffusion information contained in the tensor. Our first multivariate method uses the Hotelling's  $T^2$  statistic and the second uses linear discriminant analysis to generate the linear discriminant function at each voxel to form a *separability metric*. Both multivariate methods confirm the findings from the individual metrics of large-scale changes in the bilateral inferior temporal gyri of the boxers, but they also reveal greater sensitivity as well as identifying major subcortical changes that had not been evident in the univariate analyses. Linear discriminant analysis has the added strength of providing a quantitative measure of the relative contribution of each metric to any differences between the two subject groups. This novel adaptation of statistical and mathematical techniques to neuroimaging analysis is important for two reasons. Clinically, it develops the findings of a previous mild head injury study, and, methodologically, it could equally well be applied to multivariate studies of other pathologies.

© 2008 Elsevier Inc. All rights reserved.

**Keywords:** Multivariate analysis; Voxel-based analysis; Linear discriminant analysis; Diffusion tensor imaging; Separability metric; Mild repetitive head injury; Hotelling's  $T^2$  statistic

## 1. Introduction

Conventional neuroimaging analysis such as that performed by Statistical Parametric Mapping (SPM) [1] employs univariate statistics. Multivariate methodology using multiple biomarkers may improve the sensitivity of significance testing between groups of subjects and controls to provide a more sensitive indication of regions of brain damage. To test this hypothesis, two multivariate methods were applied to diffusion tensor imaging (DTI) data obtained from professional boxers who had experienced chronic, mild, closed head injury, for which the results from standard univariate analysis have been published elsewhere [2].

DTI is a valuable tool to identify microscopic changes in brain tissue resulting from damage or disease [2–6]. The  $3 \times 3$  symmetric tensor that models the diffusion of water in the brain can be represented geometrically by an ellipsoid [7]. The tensor contains information about the ellipsoid's axes lengths and spatial orientation. The axis lengths are proportional to the square roots of the three tensor eigenvalues,  $\lambda_1 \geq \lambda_2 \geq \lambda_3 \geq 0$ . If the ellipsoid's three orthogonal axes are aligned with the reference axes, the tensor is diagonal; if the ellipsoid is rotated with respect to the reference axes, the tensor contains symmetric off-diagonal elements to account for the rotation. Several tensor derivatives are unaffected by any rotation of the tensor, and these are the quantities used to calculate quantitative values of the diffusion process [8–10]. Such derivatives that are potentially useful for imaging can be classified into three groupings: *apparent diffusion coefficients*, which measure

\* Corresponding author. ISB/MR-Senter, St Olavs Hospital, 7006 Trondheim, Norway. Tel.: +47 7386 9553; fax: +47 7386 7708.

E-mail address: [michael.chappell@ntnu.no](mailto:michael.chappell@ntnu.no) (M.H. Chappell).

the “magnitude” of the diffusion; *diffusion anisotropy indices*, which measure the directional preferences of the diffusion; and the *apparent propagation measures*, which quantify whether the geometry of the diffusivity is more linear ( $\lambda_1 \geq \lambda_2 \approx \lambda_3$ ), spherical ( $\lambda_1 \approx \lambda_2 \approx \lambda_3$ ) or planar ( $\lambda_1 \approx \lambda_2 \geq \lambda_3$ ). Diffusion following a single fibre bundle shows linear diffusivity, while regions of crossing fibres, along with any sheet-like structures, show planar diffusivity [11]. Since these three groupings are measuring different physical properties of diffusion, it is conceivable that they might be sensitive to different microstructural changes. To ignore two of the three groupings, as is necessary in conventional univariate analysis, risks losing important information about such changes.

In this study, mean diffusivity (MD) was used as the apparent diffusion coefficient; fractional anisotropy (FA) as the diffusion anisotropy index; and mode as the apparent propagation measure. In terms of the tensor eigenvalues, these are given by:

$$\text{MD} = \frac{1}{3}(\lambda_1 + \lambda_2 + \lambda_3) \quad (1)$$

$$\text{FA} = \sqrt{\frac{3}{2} \frac{(\lambda_1 - \text{MD})^2 + (\lambda_2 - \text{MD})^2 + (\lambda_3 - \text{MD})^2}{\lambda_1^2 + \lambda_2^2 + \lambda_3^2}} \quad (2)$$

$$\text{mode} = \frac{\lambda_1 \lambda_2 \lambda_3}{\left[ (\lambda_1 - \text{MD})^2 + (\lambda_2 - \text{MD})^2 + (\lambda_3 - \text{MD})^2 \right]^{3/2}} \quad (3)$$

Voxel-based analysis of brain structure, such as that done by SPM, leaves the choice of the variable of interest to the individual researcher. The analysis is, however, restricted to being univariate. Commenting on this aspect of the methodology in their paper on voxel-based morphometry (using grey matter concentration as the variable of interest), Ashburner and Friston [12] said, “A possibly more powerful procedure would be to use some form of voxel-wise multivariate approach...The Hotelling’s  $T^2$  test could be used to perform simple comparisons between two groups. However, for more complex models, the more general multivariate analysis of covariance would be necessary.” This study picks up this suggestion from morphometry and applies it to the investigation of microstructural integrity, using the same underlying methodology. Here, instead of using grey matter concentration as in morphometric analysis, we use the diffusion tensor derivatives MD, FA and mode. To our knowledge, it is the first time that microstructural integrity has been interrogated using multivariate methods with voxel-based DTI parameters.

Our first multivariate method entailed evaluating the Hotelling’s  $T^2$  statistic [13,14] at each voxel to test the null hypothesis that the centroid (the vector of means of the three metrics) of the boxer dataset was the same as the centroid of

the control dataset. This statistic is the multivariate counterpart of Student’s  $t$ -statistic, while the centroid is the multivariate counterpart of the mean.

Our second method was a novel application of linear discriminant analysis (LDA) at the voxel level. Other studies have used LDA to investigate brain structure, but they focused on using LDA to perform group identification, such as one based on regional DTI data [15] and another using multimodal MR spectroscopic and conventional MRI data [16]. The aim of the approach used in this report was to employ LDA at every single voxel to generate a new diffusion metric to subsume independent MD, FA and mode measures, to maximise the differentiation between the group of boxers and their controls at the level of each voxel. We called this new metric the *separability metric*. The feature of this approach compared with other multivariate analyses is that it is voxel based, generating this new separability metric at each voxel. The advantages of a voxel-based approach over operator-dependent region selection are well documented (see, e.g., [17]). In this way, it can be used to investigate every voxel, and to objectively identify those where the separability metric of the boxers is statistically significantly different from the controls. To do this, the new metric was used in a standard voxel-based analysis of the brain using SPM2 (<http://www.fil.ion.ucl.ac.uk/spm/>). The difference between this approach and standard SPM analysis is that instead of using MD, FA or mode individually in the analysis, the separability metric has, at each voxel, incorporated information from all three diffusion metrics to ensure optimal separability between the two groups of subjects. Extending the improved power of multivariate analysis to DTI data at the voxel level is likely to have potential value in studying many clinical disorders that involve diffuse and/or multisystem alterations or damage.

## 2. Materials and methods

In vivo data were acquired from 59 professional male boxers and 12 male control subjects (aged from 22 to 31 years) in the same age range. The control subjects were free from neurological disease and had no boxing history. Informed consent was obtained from all participants. Imaging protocols were approved by the institutional review board. The brain imaging was part of a screening programme to monitor professional boxers; those in this study did not show clinical signs of neurological damage. Conventional MR imaging of these subjects produced negative or nonspecific findings, including cavum septum pellucidum, subcortical white matter disease and periventricular white matter disease.

### 2.1. MR Data acquisition

Scans were performed on two GE 1.5-T MRI scanners (General Electric Medical Systems, Milwaukee, WI, USA)

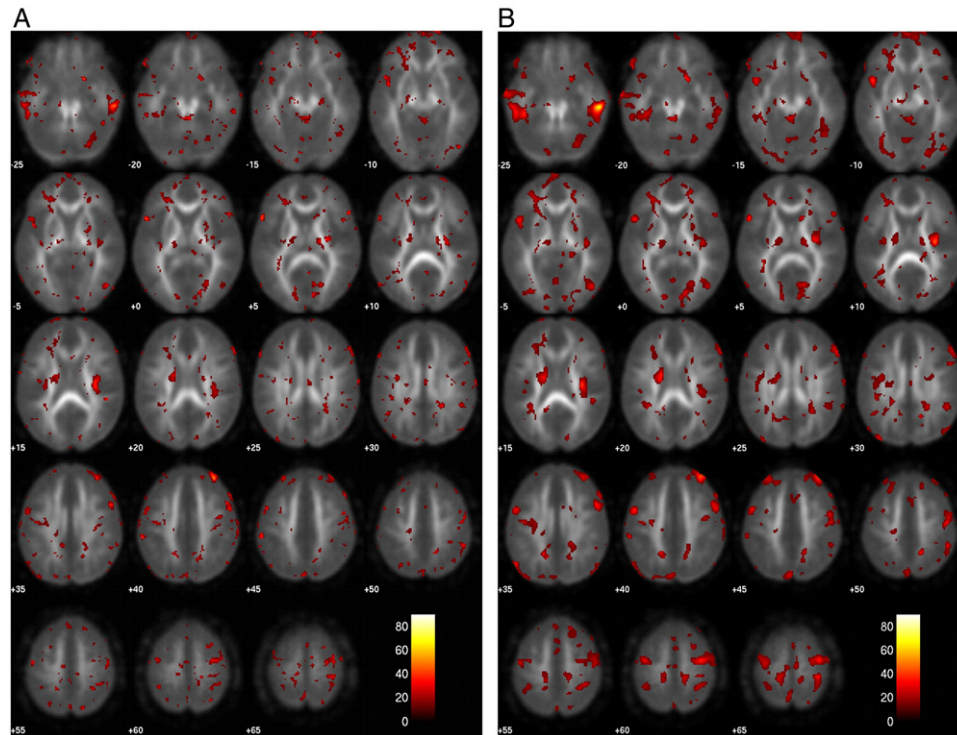


Fig. 1. Comparison of the effects of different smoothing filters. Statistical group comparisons and data used in each case were identical, except for the isotropic filter width of (A) 4 mm and (B) 8 mm FWHM.

with 22 mT/m gradient strength. A quadrature head coil was used, and in all cases the section thickness was 5 mm, with no intersection gaps. A 2D spin-echo EPI acquisition was used with TE/TR=100 ms/12 s. An acquisition matrix of  $128 \times 128 \times 30$  and  $1.7 \times 1.7 \times 5$  mm<sup>3</sup> voxels in 26 gradient directions with direction-dependent  $b$  values between 815 and 1152 s/mm<sup>2</sup>, and six acquisitions with no diffusion weighting, was used. The total acquisition time was 6 min 24 s. No subjects, whether boxers or controls, were excluded from the analysis.

SPM2 was used to preprocess the data. The images were firstly spatially normalized to the Montreal Neurological Institute's (MNI) EPI template using SPM's nonrigid body transformations. The source image used to obtain the normalization parameters for each subject was the subject's T2-weighted ( $b=0$  s/mm<sup>2</sup>) image which was fitted to an MNI template image with similar contrast. These parameters were applied to the MD, FA and mode images. The resulting normalized images were then smoothed. The selection of the smoothing filter width should ideally be driven by the matched filter theorem, which states that the filter width should match the expected size of the differences being investigated [18,19]. In practice, however, this a priori information is seldom available. However, as traumatic head injury is known to manifest itself as diffuse axonal injury [20,21], we started with a 4-mm full-width at half maximum (FWHM) filter and compared it with an 8-mm one (Fig. 1). This visual comparison showed the 8-mm filter was more sensitive and was thus used in all remaining analyses. It is

also an intermediate width in the range of 0–16 mm reported in the literature [18].

The pre-processed normalized, smoothed images became the input data for all three analysis methods: conventional univariate testing, Hotelling's  $T^2$  statistic and the LDA. Multiple comparison correction algorithms such as false discovery rate and random field theory corrections have not yet been written for the Hotelling's algorithm. To facilitate comparison of the different methods, we therefore addressed the problem of multiple comparisons by using a level of significance for the two-tailed  $t$  tests of  $\alpha=0.001$ , and by requiring a cluster size of at least  $k=8$  voxels before the cluster was accepted. A flowchart outlining the analysis methods used is shown in Fig. 2.

## 2.2. Hotelling's multivariate tests

We used Hotelling's  $T^2$  statistic to perform multivariate hypothesis tests of the data (see Johnson and Wichern [22] for the relevant equations). With this methodology, an imbalance in the "strengths" of the contributing metrics tends to reduce the power of the final test compared to the strongest individual metric. In this study, including the weak metric mode was found to noticeably reduce the power of the analysis. We therefore opted to use just MD and FA in the Hotelling's analyses in this study.

## 2.3. Linear discriminant analysis

Linear discriminant analysis (see [23,24]) investigates the extent to which two or more groups of subjects can be

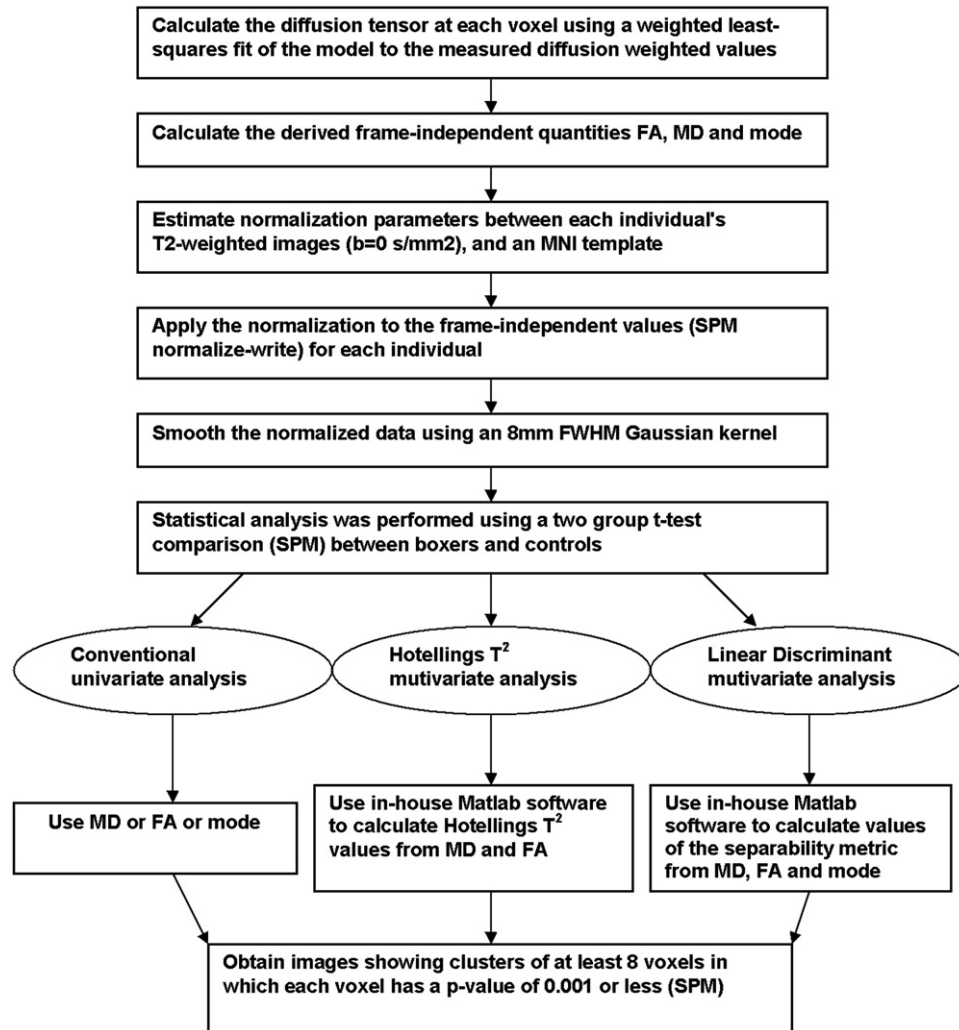


Fig. 2. Flowchart outlining the analysis process from using the DTI data to find the tensor at each voxel through to obtaining images of statistical difference between the subject and control groups.

separated, based on the measurements of several different variables for each subject. It does this by maximizing the ratio of the between-group variance to the within-group variance — i.e., the distance between the groups is maximized while the distance within the groups is minimized. The resulting “separating” function is called the *linear discriminant function*. Unlike Hotelling’s analysis, LDA does not penalise strong metrics if weaker ones are included in the analysis. This is because it finds the weighted combination of the metrics that best separates the two groups. Any metric that contributes little or nothing to the discriminating power of the analysis is simply down- or zero-weighted.

If  $x_i$  are the univariate metrics being used (in this study MD, FA and mode), the linear discriminant function ( $L$ ) can be written as

$$L = a_0 + a_1x_1 + a_2x_2 + \dots + a_nx_n. \quad (4)$$

The weighting parameters  $a_i$  are determined in such a way that the discrimination between the groups is maximised. The

linear discriminant function is the single linear function in MD, FA and mode that provides a mathematically derived optimal discrimination between the boxer and control groups. This is the justification for using the evaluated linear discriminant function for each subject at each voxel as the new multivariate metric to test for differences between boxers and controls, and to test whether it is more sensitive than any of the contributing univariate metrics.

We used the Fisher’s Linear Discriminant function in the Matlab Statistical Pattern Recognition toolbox<sup>1</sup> to perform the LDA. Its identification of the function that best discriminates between the groups is based on the Rayleigh quotient as the measure of separability [25].

The novelty of this study is in applying LDA to each and every voxel, and thus generating a different linear discriminant function at each voxel. This provides two important pieces of information about that voxel. Firstly, it

<sup>1</sup> <http://cmp.felk.cvut.cz/~xfrancv/stprtool/>.

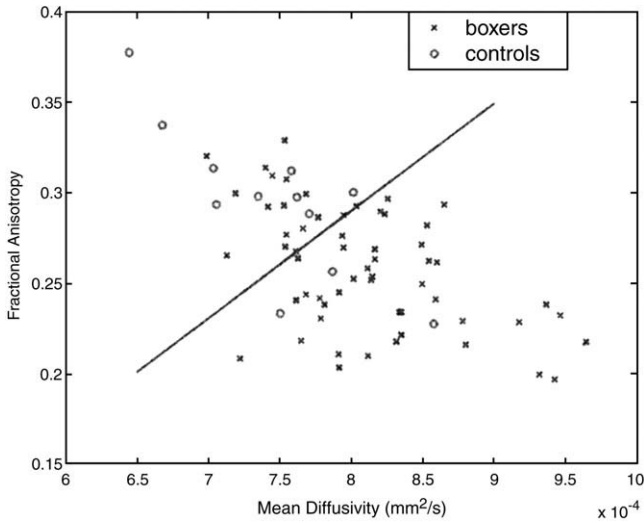


Fig. 3. Scatter plot of FA vs. MD for voxel with MNI coordinates (36 –16 12) in the insular cortex. The linear discriminant function using the FA and MD metrics (the “separator line”) is superimposed. For ease of display and visualisation, this result was produced using only two of the three metrics, with an attendant reduction in successfully categorising each subject from 90% to 72%.

finds the linear discriminant function  $L$ , which is the linear combination of the three metrics that best separates boxers from controls at that voxel. This gives a quantitative measure of the discriminating ability of the different contributing metrics at that voxel — i.e., which metrics contribute most to the separation. This property is the motivation for the novel use of LDA in this study: that a *separability metric* can be generated at each voxel of each subject. This is done by the voxel-wise evaluation of  $L$  for each subject. These separ-

Table 1

A pair-wise comparison of the sensitivity of the different methods, where the number of “significant” voxels common to both methods as a proportion of the total number of voxels in the brain is recorded (For example, the number of voxels that were identified as significant by both univariate MD and by Hotelling’s  $T^2$  comprised 1.8% of the brain)

	Univariate MD	Hotelling’s $T^2$	Linear discriminant analysis
Univariate MD	0.040	0.018	0.023
Hotelling’s $T^2$	0.018	0.050	0.031
Linear discriminant analysis	0.023	0.031	0.126

ability metric values for each subject were then used in significance testing to find voxels where the boxers’ and controls’ values were different.

An example of the results of LDA at a single voxel in the insular cortex region [with MNI coordinates (36 –16 12)] is shown in Fig. 3. This scatterplot shows the expected pattern that with mild head injury MD increases and FA decreases [26,27]. With the diffusion metric values statistically normalized to a mean of 0 and standard deviation of 1, the discriminant function (Eq. (4)) for this voxel was:

$$L = 0.0265 + 0.0116 \times MD_z - 0.0042 \times FA_z - 0.038 \times mode_z$$

where the  $z$  subscript refers to normalized values. The coefficients show that at this voxel mode is the strongest metric, followed by MD, with FA the weakest. This is unusual, as mode is typically a weak discriminator (see Results and discussion section below) which is not used in univariate analysis. However, in the rare voxels such as this one where it makes an important contribution to the

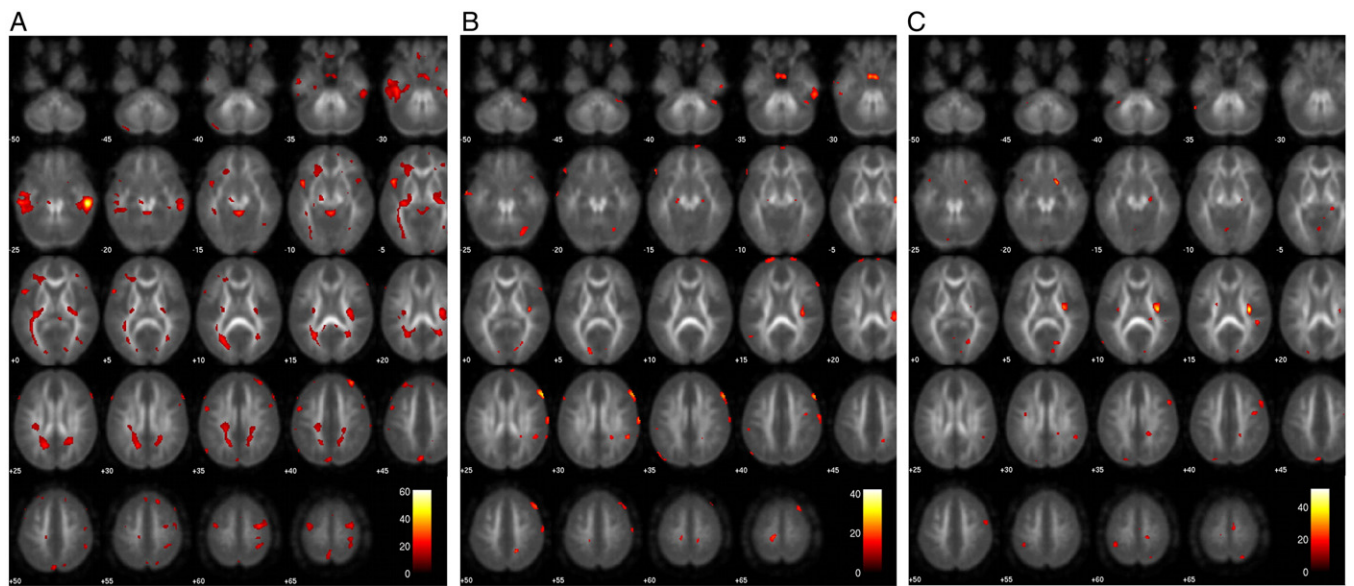


Fig. 4. Coloured regions showing voxels where the boxers are statistically significantly different from the controls ( $\alpha=0.001, k=8$ ). These regions are superimposed on an average FA map of normalized, undamaged brain. The univariate analyses used are (A) MD, (B) FA and (C) mode.

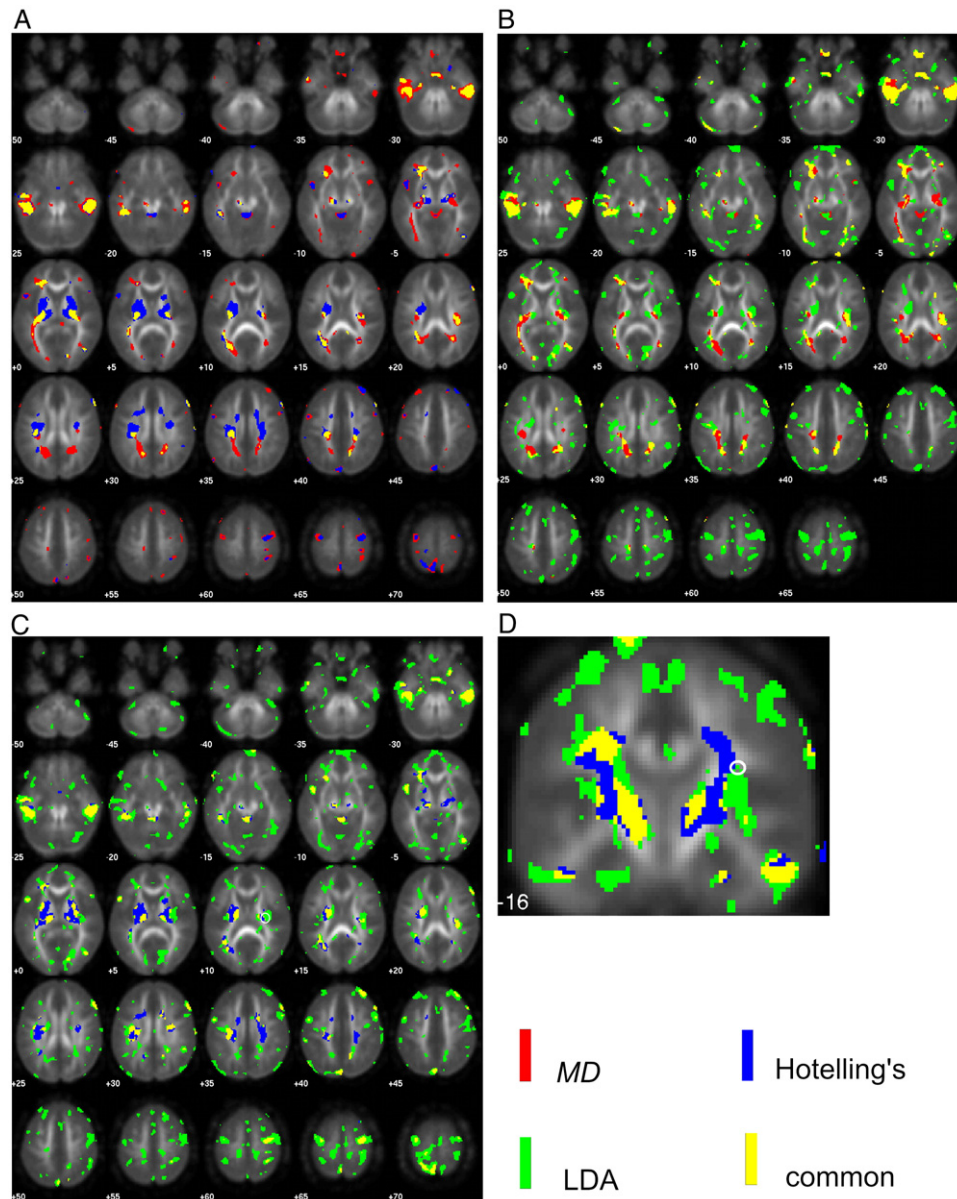


Fig. 5. Coloured regions showing pair-wise comparisons of where each method identifies the boxers as being statistically significantly different from the controls, and where the two methods overlap ( $\alpha=0.001$ ,  $k=8$ ), using (A) univariate MD vs. Hotelling's  $T^2$  statistic from MD and FA; (B) univariate MD vs. LDA's measure using MD, FA and mode; (C) Hotelling's  $T^2$  statistic from MD and FA, vs. LDA's measure using MD, FA and mode; and (D) a coronal section of the main damage identified by both Hotelling's and LDA methods. These regions are superimposed on an average FA map of normalized, undamaged brain. The circled regions (C and D) contain voxel (36 -16 12) (see also Fig. 3), whose analysis is discussed in the text.

ability to discriminate between the two groups, LDA is able to include this information and so increase the power of the test. This illustrates the importance of the linear discriminant function as a separator, optimally incorporating as it does, separation information from all three metrics at every voxel.

### 3. Results and discussion

Before utilising multivariate analyses, it is important to understand the behaviour of the three univariate metrics

separately. Fig. 4 displays standard two-sample two-tailed  $t$ -test results for each metric. Visual inspection shows that overall there is one strong metric (MD) and two weak ones (FA and mode) in identifying differences between the professional boxer brains and the control brains.

The comparative sensitivities of Hotelling's, LDA and the univariate MD methods in this study are shown in Table 1. This quantifies the extent of the regions identified as being different between boxers and controls by the different methods. From the table, it is apparent that LDA is 2.5 times as sensitive as Hotelling's, which itself is 1.25 times as sensitive as MD. The Hotelling's linear discriminant pairing

has the greatest overlap, i.e., the greatest number of “significant” voxels in common, with Hotelling’s sharing 60% of its significant voxels with LDA.

Fig. 5 shows the pair-wise comparisons of the regions of difference unique to each method, and the regions common to both. Fig. 5A shows that Hotelling’s  $T^2$  confirms the main problem area identified by MD: bilateral damage to the region of the inferior temporal gyrus. In addition, however, the Hotelling’s approach identifies major subcortical damage in the striatum and thalamus that was not detected by MD. By contrast, Hotelling’s did not detect some of the diffuse white matter damage shown by MD.

Fig. 5B and C shows that LDA appears to provide an optimal multivariate approach. LDA supports the main damage identified by both the univariate MD analysis and the multivariate (MD and FA) Hotelling’s analysis, although the extent of subcortical damage in the striatum and thalamus is less evident. An additional feature of the LDA analysis is that it reveals more diffuse microstructural damage than the other methods. Fig. 5D is a coronal view of the damage to the subcortical and internal capsule regions, showing that the subcortical damage in boxers appears most prominent at the level of the posterior limb of the internal capsule when analysed with Hotelling’s and LDA multivariate methodologies. This finding, not apparent from the univariate analysis of these data, is in agreement with results of another boxers study [28].

#### 4. Conclusions

In this study, we have presented two different methods for analysing and displaying differences in brain structure between two subject groups using multivariate statistics. The two methods are the voxel-wise evaluation of Hotelling’s  $T^2$  tests of multivariate data and Student’s  $t$  tests of LDA’s separability metric that optimises group differences at individual voxels.

In this study, LDA was more sensitive and provided more detail of the microstructural damage in the boxers, while Hotelling’s statistic revealed fewer, more consolidated subcortical clusters. LDA in addition reflects the diffuse nature of the mild, repetitive, closed head injury. Hotelling’s and LDA methods complement each other, improving the power and thereby extending the findings of separate univariate analyses.

LDA is robust to changes in the relative strengths of the contributing metrics, since if one metric is weak at a particular voxel, it is down-weighted there without penalising the others. This is a strength it has over the Hotelling’s method which loses power when a weak metric is included. We have demonstrated LDA’s flexibility in this regard, showing how it can capture the discriminating information from a metric that is weak in most voxels but is nevertheless a strong separator in a few.

A weakness of this retrospective study is the low number of control subjects, which considerably reduces the power of the analyses. Despite this limitation, these new methods enabled us to identify major subcortical damage in the brains of the professional boxers that was not evident using univariate analysis.

#### References

- [1] Worsley KJ, Marrett S, Neelin P, Vandal AC, Friston KJ, Evans AC. A unified statistical approach for determining significant signals in images of cerebral activation. *Hum Brain Mapp* 1996;4(1):58–73.
- [2] Chappell MH, Ulug AM, Zhang L, Heitger MH, Jordan BD, Zimmerman RD, et al. Distribution of microstructural damage in the brains of professional boxers: a diffusion MRI study. *J Magn Reson Imaging* 2006;24(3):537–42.
- [3] Lee ZI, Byun WM, Jang SH, Ahn SH, Moon HK, Chang YM. Diffusion tensor magnetic resonance imaging of microstructural abnormalities in children with brain injury. *Am J Phys Med Rehabil* 2003;82(7):556–9.
- [4] Pfefferbaum A, Sullivan EV. Microstructural but not macrostructural disruption of white matter in women with chronic alcoholism. *NeuroImage* 2002;15(3):708–18.
- [5] Huppi PS, Murphy B, Maier SE, Zientara GP, Inder TE, Barnes PD, et al. Microstructural brain development after perinatal cerebral white matter injury assessed by diffusion tensor magnetic resonance imaging. *Pediatrics* 2001;107(3):455–60.
- [6] Klingberg T, Hedehus M, Temple E, Salz T, Gabrieli JDE, Moseley ME, et al. Microstructure of temporo-parietal white matter as a basis for reading ability: evidence from diffusion tensor magnetic resonance imaging. *Neuron* 2000;25(2):493–500.
- [7] Basser PJ, Mattiello J, LeBihan D. Estimation of the effective self-diffusion tensor from the NMR spin-echo. *J Magn Reson Series B* 1994;103(3):247–54.
- [8] Ennis DB, Kindlmann G. Orthogonal tensor invariants and the analysis of diffusion tensor magnetic resonance images. *Magn Reson Med* 2006;55(1):136–46.
- [9] Kingsley P. Introduction to diffusion tensor imaging mathematics: Part II. Anisotropy, diffusion-weighting factors, and gradient encoding schemes. *Concepts Magn Reson Part A* 2006;28A(2):123–54.
- [10] Westin CF, Maier SE, Mamata H, Nabavi A, Jolesz FA, Kikinis R. Processing and visualization for diffusion tensor MRI. *Med Image Anal* 2002;6(2):93–108.
- [11] Zhang S, Demiralp C, Laidlaw DH. Visualizing diffusion tensor MR images using streamtubes and streamsurfaces. *IEEE Trans Vis Comput Graph* 2003;9(4):454–62.
- [12] Ashburner J, Friston KJ. Voxel-based morphometry — The methods. *NeuroImage* 2000;11(6):805–21.
- [13] Hotelling H. A generalized T measure of multivariate dispersion. *Ann Math Stat* 1947;18(2):298.
- [14] Siotani M. On the distribution of Hotelling’s  $T^2$ -test. *Ann Inst Stat Math* 1956;8:1–14.
- [15] Lin FC, Yu CS, Jiang TZ, Li KC, Zhu CZ, Zhu WL, et al. Discriminative analysis of relapsing neuromyelitis optica and relapsing-remitting multiple sclerosis based on two-dimensional histogram from diffusion tensor imaging. *NeuroImage* 2006;31(2):543–9.
- [16] Galanaud D, Nicoli F, Chinot O, Confort-Gouney S, Figarella-Branger D, Roche P, et al. Noninvasive diagnostic assessment of brain tumors using combined in vivo MR imaging and spectroscopy. *Magn Reson Med* 2006;55(6):1236–45.
- [17] Good CD, Johnsrude IS, Ashburner J, Henson RNA, Friston KJ, Frackowiak RSJ. A voxel-based morphometric study of ageing in 465 normal adult human brains. *NeuroImage* 2001;14(1):21–36.
- [18] Jones DK, Symms MR, Cercignani M, Howard RJ. The effect of fiber size on VBM analyses of DT-MRI data. *NeuroImage* 2005;26(2):546–54.

- [19] Rosenfeld A, Kak AC. Digital picture processing. 2nd ed. New York: Academic Press; 1982. p. 42.
- [20] Gennarelli TA, Thibault LE, Graham DI. Diffuse axonal injury: an important form of traumatic brain damage. *Neuroscientist* 1998;4(3): 202–15.
- [21] Meythaler JM, Peduzzi JD, Eleftheriou E, Novack TA. Current concepts: diffuse axonal injury-associated traumatic brain injury. *Arch Phys Med Rehabil* 2001;82(10):1461–71.
- [22] Johnson R, Wichern D. Applied multivariate statistical analysis. 4th ed. Upper Saddle River: Prentice-Hall, Inc; 1999.
- [23] Johnson D. Applied multivariate methods for data analysts. London: Duxbury Press; 1998.
- [24] Manly BFJ. Multivariate statistical methods. 3rd ed. New York: Chapman & Hall/CRC; 2004.
- [25] Vojtech F, Vaclav H. Statistical pattern recognition toolbox for Matlab. Prague, Czech Republic: Center for Machine Perception, K13133 FEE Czech Technical University; 2004. [Report nr CTU-CMP-2004-08. 105 p.].
- [26] Inglese M, Makani S, Johnson G, Cohen BA, Silver JA, Gonen O, et al. Diffuse axonal injury in mild traumatic brain injury: a diffusion tensor imaging study. *J Neurosurg* 2005;103(2):298–303.
- [27] Salmond CH, Menon DK, Chatfield DA, Williams GB, Pena A, Sahakian BJ, et al. Diffusion tensor imaging in chronic head injury survivors: correlations with learning and memory indices. *NeuroImage* 2006;29(1):117–24.
- [28] Zhang L, Heier LA, Zimmerman RD, Jordan B, Ulug AM. Diffusion anisotropy changes in the brains of professional boxers. *Am J Neuroradiol* 2006;27(9):2000–4.